Volume 3
Number 3
May 2025
Pages 491-734

RSC Applied Polymers

rsc.li/RSCApplPolym

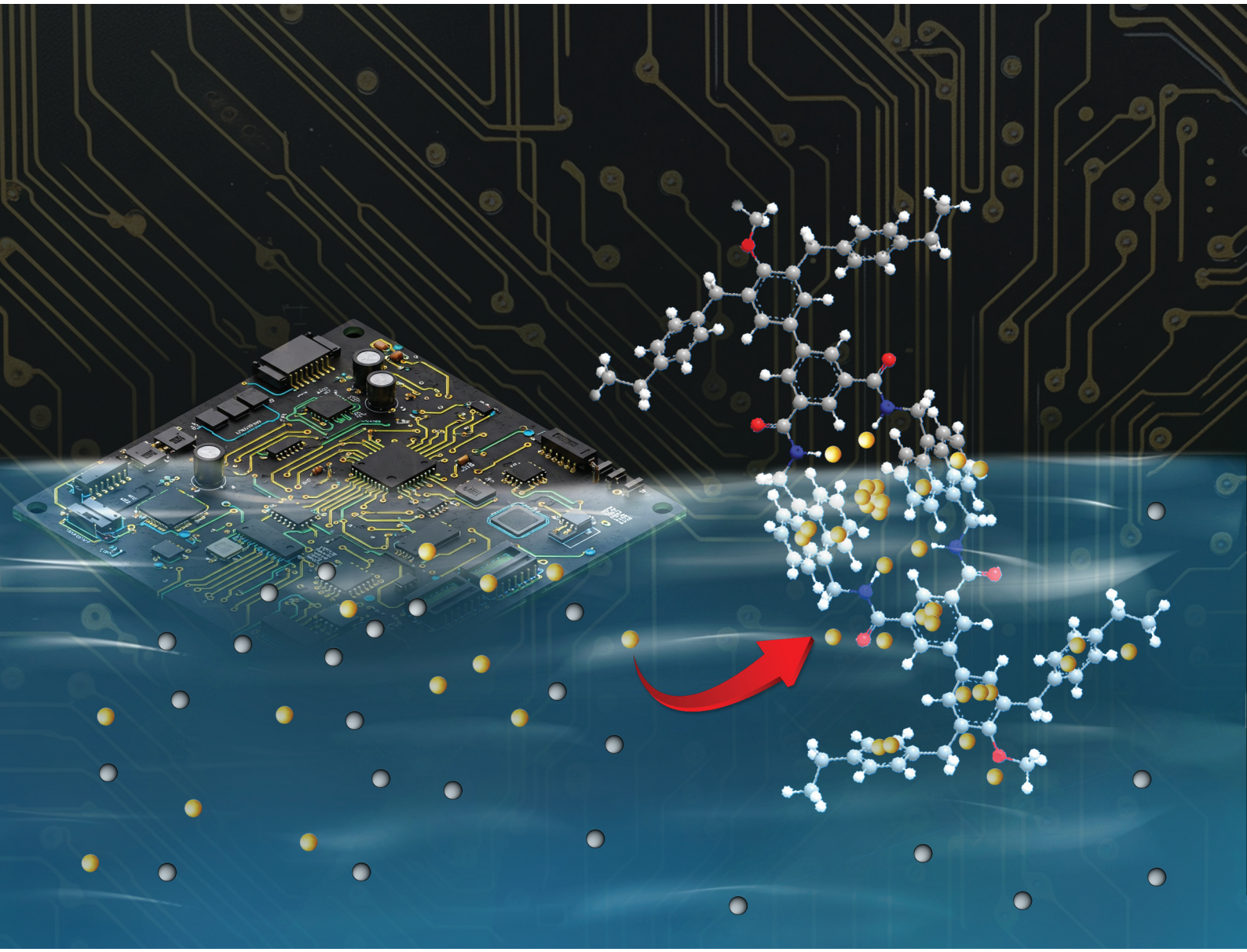

ISSN 2755-371X

ROYAL SOCIETY OF CHEMISTRY

PAPER

Jarugu Narasimha Moorthy *et al.*
Design and synthesis of tetralactam macrocycle-based porous organic polymers (POPs): application in the recovery of gold from e-waste

RSC Applied Polymers

ROYAL SOCIETY OF CHEMISTRY

PAPER

View Article Online
View Journal | View Issue

Cite this: *RSC Appl. Polym.*, 2025, **3**, 603

Design and synthesis of tetralactam macrocycle-based porous organic polymers (POPs): application in the recovery of gold from e-waste†

Ashish Kumar,‡[a] Gulshan Anjum‡[a] and Jarugu Narasimha Moorthy *[a,b]

Two porous organic polymers, **Mac-DMP** and **Mac-TMP**, based on macrocyclic tetralactam receptors for recovery of gold ions, were synthesized by the Friedel–Crafts polyalkylation reaction and characterized comprehensively. The polymer **Mac-DMP** was found to exhibit better porosity, as revealed by its BET surface area of 130 $m^2\ g^{-1}$, than **Mac-TMP**, which exhibited 26 $m^2\ g^{-1}$. The metal ion binding studies based on ICP-MS analysis, XPS studies and PXRD reveal high selectivity for the capture of Au ions. While metal ions such as Mg, Al, Ni, Cu and Sn, the predominant constituents of e-waste, were found to be untouched by these POPs, Pd ions were found to be captured as well, albeit with less efficiency than gold ions. Quantitatively, the capture capabilities of **Mac-DMP** and **Mac-TMP** from a solution of gold at pH = 2 were determined to be 1.27 and 0.72 g g^{-1}, respectively. These quantities are significantly higher than the amount possible based on the binding of one gold ion in one tetralactam receptor in the polymer, attesting to the fact that the heteroatoms and aromatic surfaces extant to the polymers facilitate the binding of gold nanoparticles within the pores created by virtue of inefficient organization of the polymers. The fact that polymers can be employed for the extraction of gold from e-waste (printed circuit boards) is compellingly demonstrated. It is further shown that both polymers can be used in a recyclable manner without significant loss of their adsorption efficiencies up to three adsorption–desorption cycles. The results thus constitute the first demonstration of macrocyclic tetralactam-based polymers for gold recovery from electronic waste and illustrate the potential for further headway in the capture of metal ions in general by receptor-based POPs.

Received 1st July 2024,
Accepted 25th November 2024

DOI: 10.1039/d4lp00218k

rsc.li/rscapplpolym

Introduction

Gold, a scarce and precious metal extracted from mines, is fast becoming depleted due to its increasing use in modern high-tech fields, electronic devices, catalysis, jewelry, *etc.*[1–6] To meet the increasing demand for electronic devices, gold is constantly produced. It is also lost in the form of electronic waste (e-waste),[7,8] of which printed circuit boards (PCBs) constitute a prototype example.[9,10] E-waste is estimated to be around 50 million tons per year with a projected increase of 8.8% every year.[11] The electronic devices in which a high content of gold is used make up a major channel by which the gold is lost; for example, with the gold available from processing one ton of its ore, only 40 mobile phones are assembled. In terms of recyclability, only 10% of gold is recovered from e-waste, while 90% is recovered from jewellery.[12] About 80% of inoperative PCBs apparently go to landfills for want of procedures that permit recovery of gold selectively with high adsorption capacity and preclude cyanide-based protocols.[13] There is, thus, a compelling need to develop improved and environmentally harmless procedures that employ ecologically advantageous materials for the recovery of gold selectively from electronic waste.

Several adsorbents have been developed for capturing the gold from complex solutions of metal ions, which include modified polysaccharide adsorbents,[14,15] chelating resins,[16,17] nanoparticles,[18–20] β-cyclodextrin,[21] functionalized silica,[22] metal–organic frameworks (MOFs),[23–27] covalent organic frameworks (COFs)[28–30] and porous organic polymers (POPs).[12,31] POPs are emergent materials that have surged into prominence in view of their high thermal and chemical stability, tunable properties by the bottom-up design of building

[a]*Department of Chemistry, Indian Institute of Technology Kanpur, 208016, India. E-mail: moorthy@iitk.ac.in*
[b]*School of Chemistry, Indian Institute of Science Education and Research Thiruvananthapuram, Trivandrum 695551, India*

†Electronic supplementary information (ESI) available: Synthesis and characterization of compounds, TGA, solid-state ^{13}C NMR spectra of polymers, XPS, elemental mapping, DFT-optimized structure, ^{1}H and ^{13}C NMR spectral reproductions. See DOI: https://doi.org/10.1039/d4lp00218k

‡These authors contributed equally.

blocks and choice of reactions for polymerization and recyclability.[32,33] They are now being actively utilized in a variety of applications, which include sensing, gas adsorption, heterogeneous catalysis, separation of molecules, control of diffusion rates, *etc*.[34–52] A common approach for the development of POPs as adsorbents is to incorporate electron-rich atoms such as nitrogen, oxygen, sulfur, *etc*. as part of polymeric backbones to leverage their capability to chelate or coordinate metal ions. A few POPs have been reported for the extraction of precious metals such as Au, Pd, Pt and Ag.[12,31] In continuation of our investigations entailing rational design and development of functional materials in a bottom-up fashion,[53–56] we envisioned that POPs could be developed as sorbents for the extraction of precious gold selectively from e-waste by exploiting tetralactam receptors as building blocks. The literature search revealed that the tetralactam constructed from 2 equivalents of each of isophthalic acid and 9,10-bis (aminomethyl)anthracene exhibits high capability to capture Au(III) ions.[57] This tetralactam and analogous systems have also been exploited for encapsulation of squaraine dye,[58] intercalation of phenazine,[59] and formation of rotaxanes,[60–62] to act as an anion sensor,[63] and also used in the removal of organic micropollutants.[64] We thus designed two building blocks **Mac-TM** and **Mac-DM** based on this tetralactam, which can be subjected to Friedel–Crafts polyalkylation using *p*-xylene dichloride (Scheme 1). In addition to the fact that the gold ions can be bound in the macrocyclic receptor, the organization of polymeric chains of the POP with heteroatoms as well as aromatic surfaces extant to aromatic rings such as anthracene are also expected to facilitate *exo*-receptor binding of the metal ions. Herein, we report the synthesis of tetralactam-based POPs as well as the capture of gold selectively by thus designed POPs. It is noteworthy that the results constitute the first example of a POP based on the tetralactam macrocycle for the recovery of precious metals from e-waste and mixed-metal solutions.

Experimental section

The derivatives of 3,5-dicarbonyl dichloride and 9,10-bis (aminomethyl)anthracene were obtained by following the reported methods. 9,10-Bis(aminomethyl)anthracene was synthesized by the Delépine reaction of 9,10-bis(bromomethyl) anthracene. Aryl-substituted isophthalates were prepared by the Suzuki cross-coupling reaction by employing appropriately functionalized boronic acids and bromobenzene (*cf.* Schemes S1–S8).†

Synthesis of Mac-TM and Mac-DM[58]

A three-neck oven-dried 500 mL round bottom flask was charged with 300 mL of dry dichloromethane under a nitrogen atmosphere. Two solutions were prepared separately; one was that of a 3,5-dicarbonyl dichloride derivative (2′,6′-dimethyl-[1,1′-biphenyl]-3,5-dicarbonyl dichloride or 4′-methoxy-[1,1′-biphenyl]-3,5-dicarbonyl dichloride) (113 mg, 0.37 mmol) in dry DCM (25 mL), while the other was of 9,10-bis(aminomethyl)anthracene (88 mg, 0.37 mmol) along with triethylamine (0.182 mL, 1.48 mmol) in dry DCM (25 mL). Both of these solutions were added simultaneously dropwise over 8.0 h and stirred for another 4.0 h at rt. At the end of this period, DCM was removed under reduced pressure and the residue was subjected to silica gel column chromatography using chloroform and methanol (99 : 1%) to obtain the desired product.

Mac-TM. 87.0 mg (yield, 25%); Mp >250 °C; ^{1}H NMR (400 MHz, $CDCl_3$) δ (ppm) 2.02 (s, 12H), 5.47 (s, 8H), 6.21 (s, 4H), 7.11 (d, J = 6.0 Hz, 4H), 7.18 (m, 6H), 7.43–7.41 (m, 8H), 8.12 (d, J = 1.2 Hz, 2H), 8.18–8.16 (m, 8H); ^{13}C NMR (100 MHz, $CDCl_3$): δ (ppm) 21.0, 37.5, 123.4, 124.5, 126.8, 127.7, 127.9, 129.3, 130.3, 133.78, 133.9, 135.7, 139.7, 143.4, 166.1; HRMS (ESI) m/z: $[M + H]^+$ calcd for $C_{64}H_{53}N_4O_4$ 941.4061; found, 941.4061.

Mac-DM. 97.9 mg (yield, 28%); Mp >250 °C; ^{1}H NMR (400 MHz, $CDCl_3$) δ (ppm) 3.88 (s, 6H), 5.49 (s, 8H), 6.26 (s, 4H), 7.03 (d, J = 8.8 Hz, 4H), 7.44 (m, 8H), 7.7 (d, J = 7.6 Hz, 4H), 8.19 (s, 8H), 8.5 (s, 4H); HRMS (ESI) m/z: $[M + H]^+$ calcd for $C_{64}H_{49}N_4O_6$ 945.3647; found, 945.3649.

Synthesis of the polymers Mac-TMP and Mac-DMP[39]

To a solution of the macrocycle **Mac-TM**/**Mac-DM** (100 mg, 0.11 mmol) in dry DCE (30 mL), *p*-xylenedichloride (38.5 mg, 0.22 mmol) and anhydrous $FeCl_3$ (142.7 mg, 0.88 mmol) were added. The reaction mixture was stirred for 3 d at 80 °C under an inert atmosphere; the reaction mixture was cooled to rt and washed with distilled water and ethanol to remove the unreacted $FeCl_3$ and other impurities. The polymer thus obtained was activated by treatment with several solvents such as methanol, THF, chloroform, *etc*. to remove dimers, oligomers, *etc*. After this process, the resultant material was dried in an oven at 100 °C for 24 h to obtain the desired polymer **Mac-TMP**/**Mac-DMP**. The yield of **Mac-TMP** was 94.7 mg (yield, 75%), while that of **Mac-DMP** was 101.5 mg (yield, 80%).

Results and discussion

Synthesis of Mac-TMP and Mac-DMP

To begin with, the tetralactam macrocycle-based building blocks, *i.e.*, **Mac-TM** and **Mac-DM**, were synthesized by the amide-synthesis protocol[62,65] involving reactions between 2′,6′-dimethyl-[1,1′-biphenyl]-3,5-dicarbonyl dichloride or 4′-methoxy-[1,1′-biphenyl]-3,5-dicarbonyl dichloride and 9,10-bis (aminomethyl)anthracene, respectively, in dry DCM and dry Et_3N under an N_2 atmosphere for 12 h at rt (Scheme 1); the requisite precursors were synthesized by following the reported procedures. The Delépine reaction of the 9,10-bis(aminomethyl)anthracene led to the aminomethyl derivative, that is, 9,10-bis(aminomethyl)anthracene. Aryl-substituted isophthalates were prepared by the Suzuki cross-coupling reaction by employing appropriately functionalized boronic acids and bromobenzene (*cf.* Schemes S1–S10 and Fig. S1–S17).†

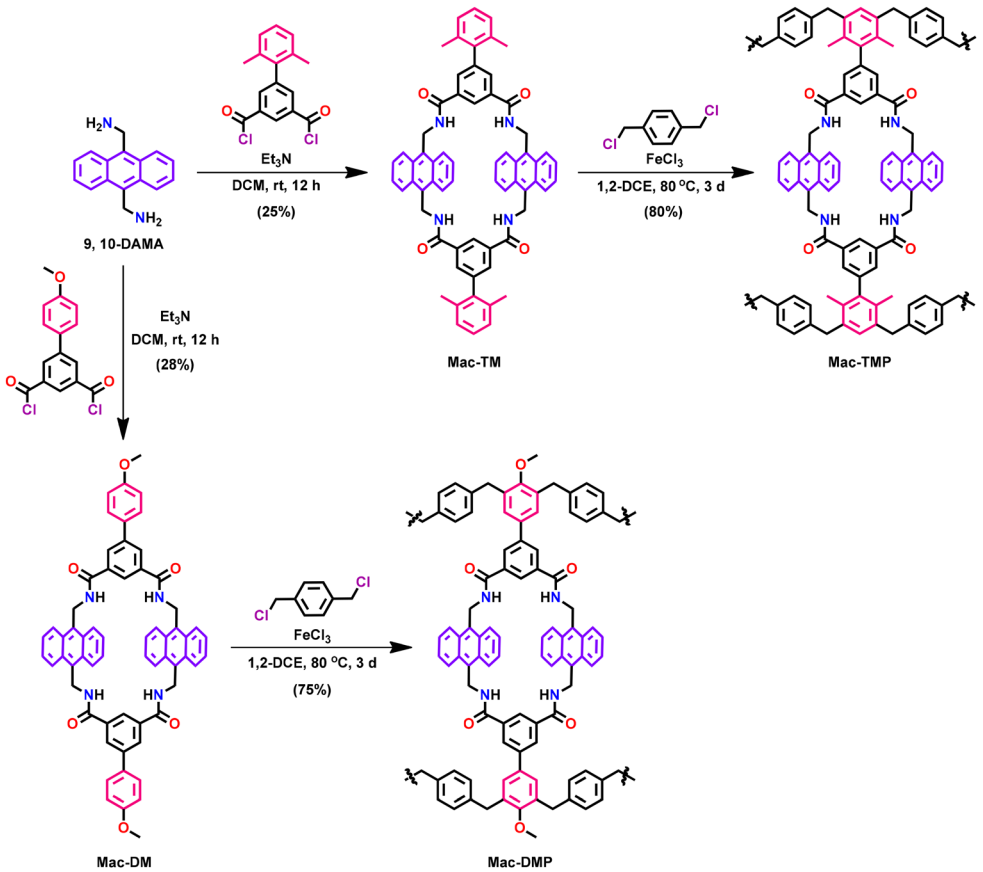

Scheme 1 Synthesis of the tetralactam macrocycle-based POPs **Mac-TMP** and **Mac-DMP**.

Subsequently, polymerization of these building blocks, *i.e.*, **Mac-TM** and **Mac-DM**, was carried out with *p*-xylene dichloride using Friedel–Crafts polyalkylation, leading to the target polymers, *i.e.*, **Mac-TMP** and **Mac-DMP**. After the polymerization, the unreacted monomers, soluble oligomers, and $FeCl_3$ were removed by thorough washing with various solvents such as methanol, THF, acetonitrile, and dichloromethane. The insoluble polymeric materials were dried in an oven at 100 °C for 24 h for further applications.

Validation of synthesized Mac-TMP and Mac-DMP

The successful synthesis of polymers **Mac-TMP** and **Mac-DMP** from the monomeric building blocks was established by Fourier-transform infrared (FT-IR) spectroscopic analysis. The IR spectra revealed absorption bands at *ca.* 3420 cm^{-1} (corresponding to the N–H stretching of the amide), 3064 cm^{-1} (attributable to the =C–H stretching), 1663–1670 cm^{-1} (corresponding to the C=O stretching), and 1505 and 1512 cm^{-1} (for the C=C and C–O stretching of the methoxy groups). The absorption for stretching of C–Cl of *p*-xylene dichloride (*p*-XDC) at 855 cm^{-1} was found to disappear in both polymers after polymerization, attesting to the fact that *p*-XDC effectively reacted as the linker (*cf.* Fig. 1a and b). The solid-state ^{13}C NMR spectra reveal the presence of different carbon atoms in the polymers; signals were observed at 166.5 and 73.3 ppm for the C=O and methylene group of $CONHCH_2$, and at 37.9 ppm for the benzylic CH_2, which attest to effective polymerization (*cf.* Fig. S18 and S19).†

Porosity, surface area, functional groups and the presence of heteroatoms in polymeric materials are considered to be significant contributors to the effective capture of gold and other precious metal ions. The Brunauer–Emmett–Teller (BET) surface areas of **Mac-TMP** and **Mac-DMP** were determined as being 26 $m^2\ g^{-1}$ and 130 $m^2\ g^{-1}$, respectively, based on N_2 sorption studies. Pore size distribution (PSD) analyses of the polymers by nonlocal density functional theory (NLDFT) reveal that these polymers exhibit different pore sizes; while the pore size in **Mac-TMP** largely centers around 2.0 nm, that in the case of **Mac-DMP** was found to vary from 1.0 to 4.0 nm, signifying the fact that **Mac-TMP** is mesoporous and **Mac-DMP** exhibits both microporous and mesoporous attributes. Due to a notable difference in the pore size distributions of the polymers, the absorption capacities are evidently different. The N_2 sorption isotherms show a gradual increase of N_2 uptake at low pressures of P/P_0 (minimal N_2 uptake) and a sharp increase at higher pressures (maximum N_2 uptake), suggesting that both polymers could be classified as type IV, according to IUPAC classification[52,66] (Fig. 1c and d). The BET analysis showed that **Mac-DMP** has a larger surface area than **Mac-TMP**; this indeed is contrary to the expectation based on the

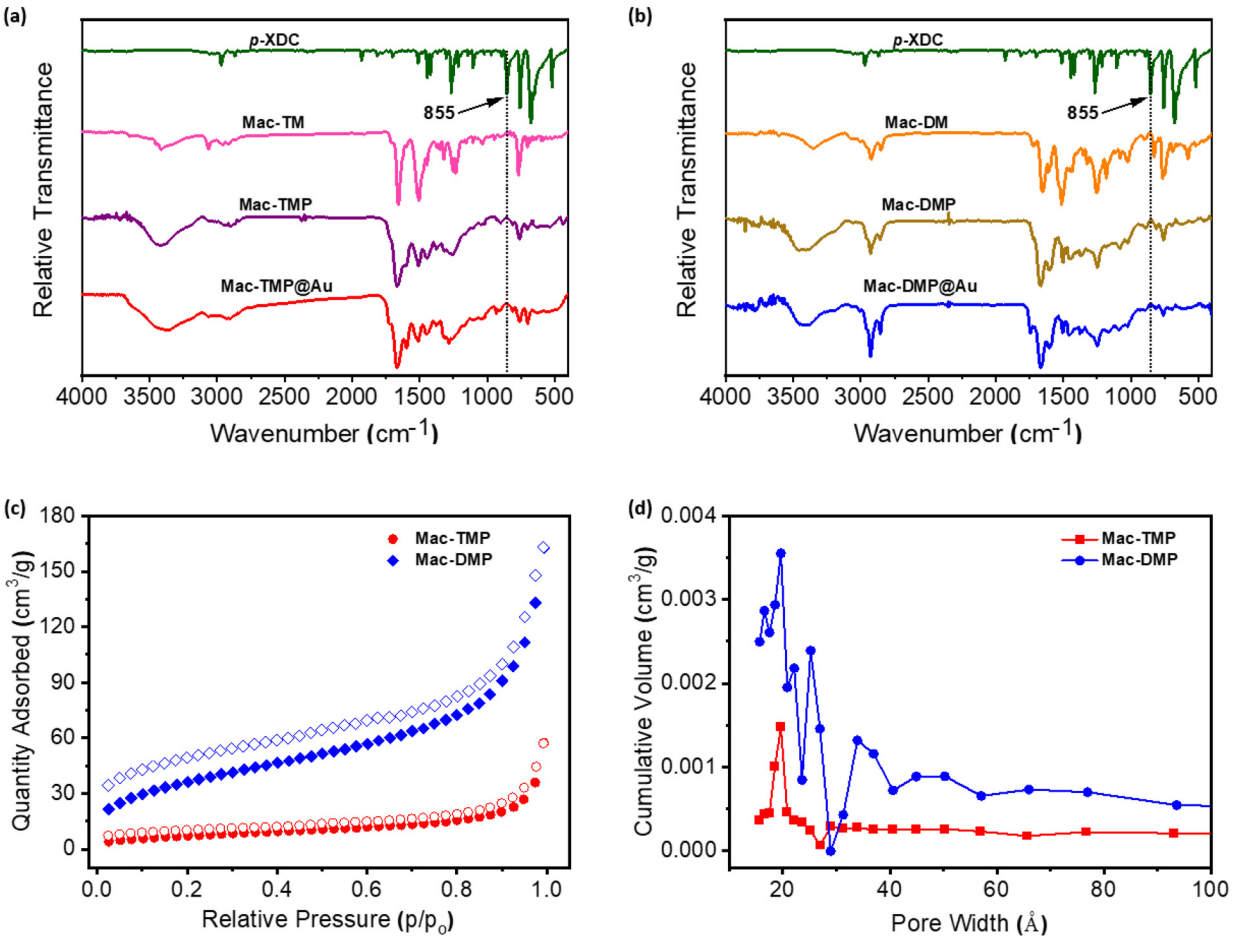

Fig. 1 (a and b) FT-IR spectra of **Mac-TMP** and **Mac-DMP**, respectively. (c) N_2 adsorption–desorption isotherms at 77 K (filled symbols represent adsorption points, and empty symbols represent desorption points). (d) Pore-size distribution profiles of **Mac-TMP** and **Mac-DMP**.

twisted building block, that is, **Mac-TM**, with which the POP is constructed, leading to more loosely organized polymeric strands and hence more porosity. The different surface areas of both polymers can be reconciled based on the polymerization of the biphenyl rings in different ways. The absence of substituents at the 2,6 and 2′,6′ positions of **Mac-DM** in the polymer **Mac-DMP** renders the biphenyl ring near planar. In contrast, the methyl groups at the 2′ and 6′ positions in the polymer **Mac-TMP** cause the rings to twist in a perpendicular fashion. The planar and twisted structures of both the monomers were established through density functional theory (DFT) calculations using the basis set 6-311g(d,p) and B3LYP functional (*cf.* Fig. S20).† Evidently, the methyl substituents occupy more space, contributing to the reduction of pore sizes in the case of **Mac-TMP**. SEM examinations revealed different textures for the two polymers (*cf.* Fig. 3d and g). Powder X-ray diffraction patterns of the polymers **Mac-TMP** and **Mac-DMP** show that both are amorphous in nature with a broad feature in the range of 2θ = 10 to 35° (*cf.* Fig. 2e).

With the porous attributes of tetralactam macrocycle-based polymers **Mac-DMP** and **Mac-TMP** established, the abilities of the two polymers to bind Au ions were investigated. It is well established in the literature that gold is captured in acidic media better.[12] Indeed, the pH-dependent adsorption of metal ions offers certain advantages in terms of e-waste treatment as the e-waste materials are largely digested in a strongly acidic solution. At pH below 3, the gold ions primarily exist as $AuCl_4^-$ ions. A known amount of the polymer (1.0 mg) was suspended in 1 mL solutions of $HAuCl_4$ of varying pH values with a uniform concentration (500 ppm). After being stirred for 36 h, the polymers were filtered, and the amount of Au depleted from each of the solutions was analyzed by ICP-MS analyses. As shown in Fig. 2a, Au ions were found to be completely adsorbed by both polymers from the solutions of pH = 2.0. The gold-bound polymers filtered from the solutions of pH = 2.0 were analyzed for the binding of Au ions by XPS. The XPS profiles revealed the presence of Au ions with binding energies of 85.5 ($4f_{7/2}$) and 89.4 ($4f_{5/2}$) eV for Au(III), 84.4 ($4f_{7/2}$) and 87.9 ($4f_{5/2}$) eV for Au(I), and 83.7 ($4f_{7/2}$) and 87.3 ($4f_{5/2}$) eV for Au (0), and peaks at 284.4 eV, 399.2 eV, and 530.6 eV for C 1s, N 1s, and O 1s, respectively (*cf.* Fig. 2b, c, S21 and S22).† The XPS data reveal that the gold bound in the POP exists in three different oxidation states, that is, Au(III), Au(I) and Au(0). Additionally, these polymers were analyzed by thermo-

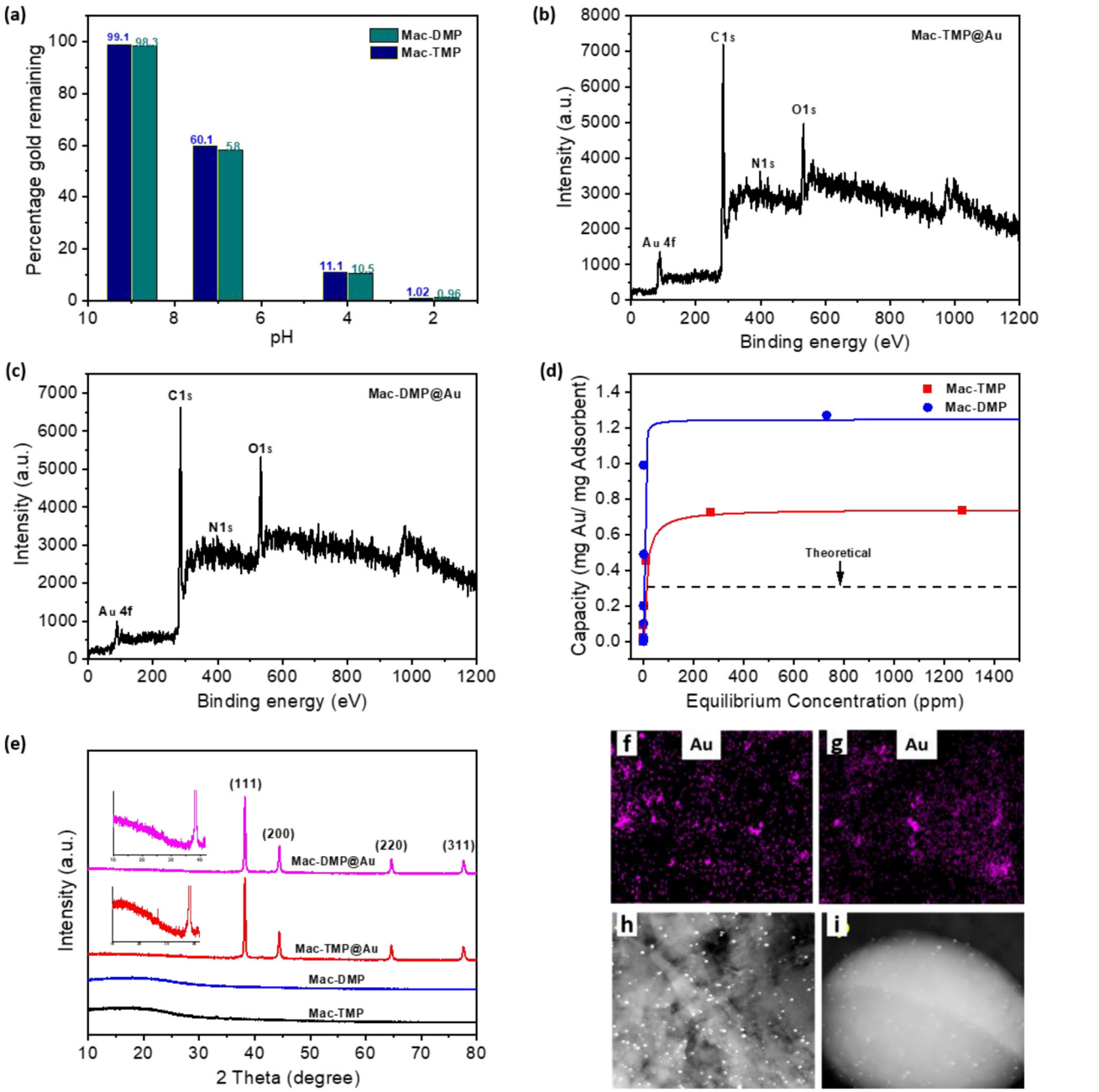

Fig. 2 (a) Ion adsorption efficiency of the polymers at different pH values. (b and c) XPS survey spectra of gold-adsorbed **Mac-TMP@Au** and **Mac-DMP@Au**, respectively. (d) Gold adsorption isotherm of **Mac-TMP** (black) and **Mac-DMP** (red) at different concentrations of 0 to 1500 ppm, and estimated theoretical limit of the adsorption based on one macrocycle binding one Au ion (dotted). (e) PXRD profiles of **Mac-TMP**, **Mac-DMP** and gold-adsorbed polymers, that is, **Mac-TMP@Au** and **Mac-DMP@Au** (inset: amorphous nature of the polymers after gold loading). (f) Elemental mapping of **Mac-TMP@Au**. (g) Elemental mapping of **Mac-DMP@Au**. (h) HAADF image of **Mac-TMP@Au**. (i) HAADF image of **Mac-DMP@Au**.

gravimetric analyses (TGA) to gauge their stabilities. The TGA profiles of **Mac-TMP@Au** and **Mac-DMP@Au** show the absence of a plateau, indicating continuous loss of mass beyond 100 °C until 300 °C. This may be attributed to the gradual decomposition of the POPs by the release of halides and associated gold ions from the polymeric matrix. Indeed, it is reported in the literature that rapid decomposition of the polymer is observed in TGA as a result of the loss of halides (*cf.* Fig. S23).†[21,26]

The adsorption capacity of each of the macrocyclic lactam-based polymers **Mac-DMP** and **Mac-TMP** was explored systematically by suspending a known amount of the polymer in $HAuCl_4$ solutions of varying concentrations at pH *ca.* 2.0; the concentrations of these solutions ranged from 20 to 2000 ppm. After stirring the POPs for 36 h in these solutions, the amount of Au adsorbed by both polymers was determined, as previously, by ICP-MS analyses. The adsorption data of both the polymers were fitted to the Langmuir adsorption isotherm

model (*cf.* Fig. 2d). To find the best adsorption isotherm model for these POPs, the experimental gold adsorption data of both polymers were fitted to Langmuir and Freundlich isotherm models, leading to better regression coefficients (R^2) for the Langmuir isotherm model of 0.9980 and 0.9908 for **Mac-DMP** and **Mac-TMP**, respectively; for the Freundlich model these coefficients were found to be 0.5922 and 0.8502 for **Mac-TMP** and **Mac-DMP**, respectively (see Fig. S24).† Thus, the Langmuir adsorption isotherm is the most suitable model to account for the adsorption of gold by **Mac-DMP** and **Mac-TMP**.

As can be seen, **Mac-DMP** exhibits saturation for the binding of Au ions at an equilibrium concentration of 1.27 g g^{-1}, while the same value is 0.72 g g^{-1} in the case of **Mac-TMP**. These gold recovery values are comparable to those of some of the polymers reported in the literature (Table S1†). It should be noted that the maximum amounts of $AuCl_4^-$ that can be bound by the polymers, based on one receptor binding with one Au ion, are 0.294 and 0.296 g g^{-1} for **Mac-DMP** and **Mac-TMP**, respectively. The experimentally observed adsorption values are significantly higher, attesting to the fact that the polymers bind Au ions not only in *endo*-receptor pockets but also in *exo*-receptor micropores formed between the polymeric strands. The polymers thus loaded with gold ions were examined by PXRD analyses, the patterns for which are shown in Fig. 2e. The PXRDs, while revealing amorphous properties of the POPs, exhibit strong diffraction peaks corresponding to Au at 2θ values of 38.1, 44.4, 64.6, and 77.6°. These correspond to the standard Bragg reflections, *i.e.*, (111), (200), (220), and (311), of the face-centred cubic lattice. The sharp peak at 38.1° indicates preferred growth in the direction of (111).[12] Clearly, these 2θ values in the PXRD patterns of the polymers correspond to elemental gold and the reduction of gold ions during adsorption, which is well documented in the literature.[67]

The average size of nanoparticles is much larger than atomic gold atoms/ions, which implies that gold forms nanoparticles on the surface of the POPs; the diameter of atomic gold is 0.296 nm, while the average size of the gold nanoparticles bound in POPs is much larger (16.34 and 7.28 nm for **Mac-TMP@Au** and **Mac-DMP@Au**, respectively); the sizes of gold nanoparticles were calculated through ImageJ software using HRTEM images. The interplanar spacing in the nanoparticles agrees well with that of the Au 111 plane (0.238 nm)[68] (*cf.* Fig. S25 and S26).† Indeed, The reduction of Au(III) during the process of adsorption and formation of clustered gold/nanoparticles has been extensively reported. Additionally, the separation of clustered gold, paving the way for more room for the adsorption of gold ions, has been invoked as one of the reasons for the high adsorption of gold by porous polymers.[69]

The nature of the distribution of gold in the polymers **Mac-TMP@Au** and **Mac-DMP@Au** was analyzed through elemental mapping and high-angle annular dark-field (HAADF) imaging of HRTEM, which shows that gold is uniformly distributed in the entire polymer material in each case (*cf.* Fig. 2f–i and S27).†

To examine the ability of POPs based on macrolactams to bind gold selectively, competition experiments were carried out with various other metal ions. For this purpose, the metal ions that are reported to be present in e-waste CPUs, namely, Mg, Al, Ni, Cu, Sn, Zn and Au, were considered. To these ions, Pd and Ag were also added. In a solution of all of these ions, each of which is present uniformly at a concentration of 100 ppm, the selective adsorption ability of the macrolactam POPs was examined. As shown in Fig. 3b, both **Mac-DMP** and **Mac-TMP** were found to bind Au ions selectively with 96 and 94% efficiencies. Rather less affinity for Pd ions was also observed with 51 and 47% efficiencies for **Mac-DMP** and **Mac-TMP**, respectively, from the solution of different metal ions. Ions such as Mg, Al, Ni, Cu and Sn were otherwise untouched with no affinity whatsoever. Zn and Ag ions were found to be bound only marginally. Thus, these studies compellingly show that Au ions are bound selectively by the macrolactam POPs.

As mentioned earlier, the amount of gold that can be adsorbed by each of the POPs, based on the assumption that one macrolactam binds one Au ion, cannot exceed 0.296 g g^{-1} of the polymer. The observed amount of gold is far greater than this limit. This attests to the fact that the gold ions and gold nanoparticles are bound in the *exo*-receptor pores of the POP. The diffraction patterns from PXRD and the presence of gold clusters in the HRTEM images of the polymers attest to the ordered arrangement of the gold and gold ions, otherwise the observed powder diffraction pattern and the amount of gold adsorbed by the polymers in far greater amounts than possible by receptor binding sites cannot be comprehended. Evidently, the heteroatoms and π-surfaces of the polymers, as presupposed, contribute to firm binding of the nanoparticles.

Extraction from e-waste. For the extraction of gold from solutions of e-waste, the e-waste (CPUs and printed circuit boards (PCBs)) was suspended in a 10 M solution of NaOH for 24 h at ambient temperature to remove the epoxy coating present on the e-waste surfaces. Subsequently, the material was removed from the NaOH solution and washed thoroughly with water and later soaked in a solution of 1.0 M HNO_3 and 1.0 M HCl (1 : 3) at rt for 2 d. The resultant solution was decanted and filtered to remove undissolved materials. The pH of the filtered e-waste solution was close to zero. Therefore, diluted aqueous solution of KOH was added to adjust the pH to *ca.* 2.0[12] (*cf.* Fig. 4). To the e-waste leached solution (5.0 mL), **Mac-DMP**/**Mac-TMP** (5.0 mg) was added in a round bottom flask, and the suspension was stirred for 36 h. Subsequently, the POP material was filtered from the resulting mixture. The amounts of different metal ions adsorbed by the polymer were analyzed by ICP-MS after extraction into an acidic thiourea solution. The adsorbed amount was determined by the standard stock solution of e-waste. The ICP-MS data showed that both polymers **Mac-DMP** and **Mac-TMP** exhibit high selectivity towards gold ions (>90%) with no binding affinity for other metal ions (*cf.* Fig. 3a). These results demonstrate the applicability of POPs as potential adsorbents for the selective capture of gold from e-waste.

What is the origin of the selective binding of Au and Pd ions? Au is selectively adsorbed by **Mac-DMP** and **Mac-TMP** from the mixture of other metal ions from e-waste along with

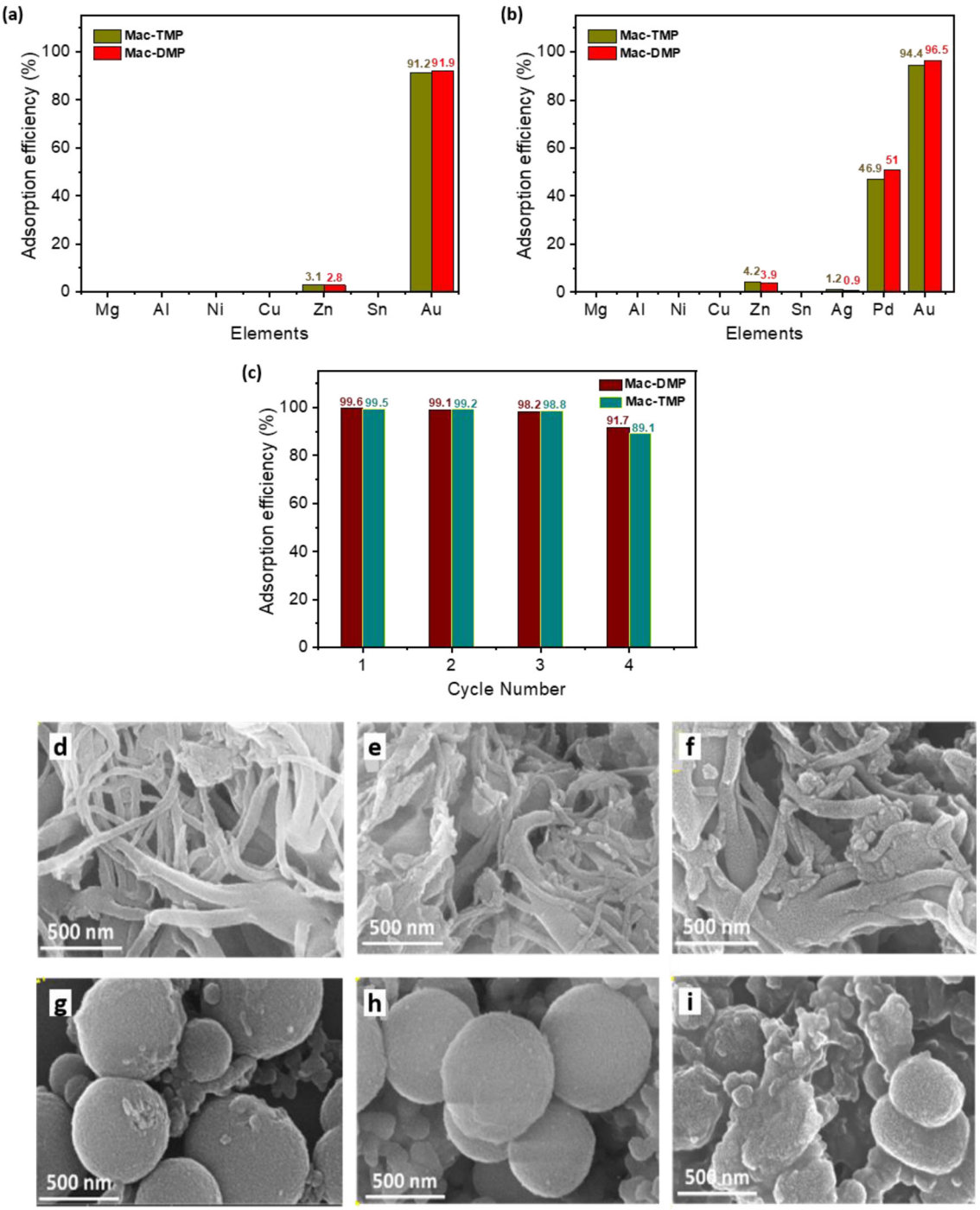

Fig. 3 (a) Percentage adsorption efficiency of gold from e-waste. (b) Competitive percentage adsorption efficiency for Au in the presence of other ions at 100 ppm. (c) Gold-adsorption efficiencies after four successive adsorption/desorption cycles. FE-SEM images of (d) **Mac-TMP**, (e) **Mac-TMP@Au**, (f) after the fourth consecutive cycle of adsorption and leaching of gold-loaded **Mac-TMP**, (g) **Mac-DMP**, (h) **Mac-DMP@Au** and (i) after the fourth consecutive cycle of adsorption and leaching of gold-loaded **Mac-DMP**.

Pd(II); indeed, the selective extraction of Au along with Pd from the mixture of a number of base metals because of their high reduction potentials is very well documented.[70] This selectivity may arise due to the fact that Au(III) and Pd(II) become negatively charged at pH = 2 and form $AuCl_4^-$ and $[PdCl_4]^{2-}$ ions, while other metal ions are positively charged. At this low pH, both the polymers may exhibit a tendency for protonation, whereby electrostatic interactions and chelation may predominate for better binding of $AuCl_4^-$ and $[PdCl_4]^{2-}$ by the polymers.[67] The square-planar structure of $AuCl_4^-$ enables its binding in the central cavity of the tetralactam core, whereby the Cl atoms of $AuCl_4^-$ may interact strongly *via* hydrogen

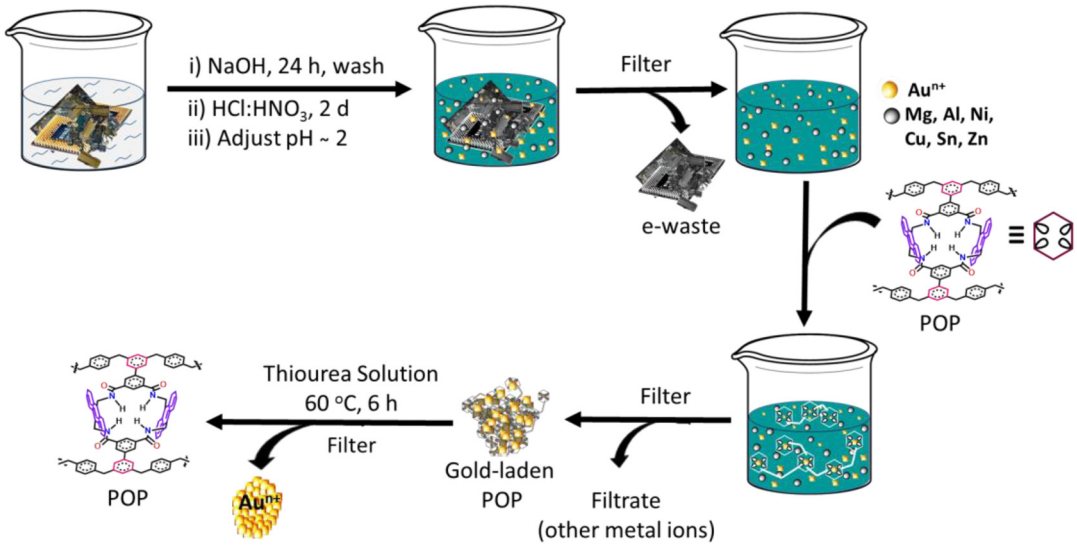

Fig. 4 Schematic illustration of the process of recovery of gold from e-waste.

bonds. The π-electrons of anthracene may also play a significant role in the selective binding of gold due to Au···π–electron interactions.[57] Overall, the adsorption of gold is governed by one or more factors such as electrostatic interactions, chelation and redox potentials. Because of the high reduction potential of $AuCl_4^-$, gold is reduced from its +3 to 0 oxidation state during the adsorption process, as mentioned above, to produce clustered gold/nanoparticles.[67] Thus, gold exists in three forms, that is, Au(III), Au(I), and Au(0), in the polymers, as evidenced by XPS, HRTEM, and PXRD.

The co-capture of gold and palladium during recovery from the e-waste in which they often co-exist can significantly affect the cost and profitability of the recovery process, especially because of the high market value of both metals. Commercially, the methods by which maximum recovery of the precious metals occurs from discarded e-waste have been implemented. Methods that effectively capture both metals obviate the need to selectively target gold or palladium separately, improving the overall recovery rate by better use of processing resources. Higher yield per batch reduces the per-unit cost of the recovery and improves revenue as both metals are valuable.

Recyclability. With the selective adsorption of gold ions by these POPs established, recyclability was explored. The desorption of gold ions is usually carried out in an acidic solution of thiourea. The gold-loaded polymers were thus suspended in acidic thiourea solutions of 0.1 M concentration and stirred at 80 °C for 6 h; gold nanoparticles, upon treatment with an acidic solution of thiourea, form a gold complex, $Au(CS(NH_2)_2)^+$, in which the Au is in its oxidation state of 1, that is, Au(I).[71,72] Subsequently, the polymers were filtered and tested for the presence of residual Au, if any, by XPS analysis; the analysis revealed that Au ions were not present. Additionally, the recovery of Au from the polymers was also analyzed by ICP-MS analysis, which revealed complete recovery. The polymers recovered after washing with distilled water, ethanol, and THF, and dried for 12 h at 100 °C were reused for binding of Au ions. The binding–desorption studies were carried out at least 3 times with a marginal diminution in the activities of the polymers. The adsorption efficiency for gold was found to decrease by 9.0%. Microscopic investigations revealed that the morphologies of the polymers changed slightly (*cf.* Fig. 3f and i).

SEM investigations were used to investigate morphological changes of the polymers with and without gold and after the leaching of the gold. The polymers **Mac-TMP** and **Mac-DMP** exhibited different morphologies, namely, long threads and spheres, respectively. While the morphologies were found to be similar after the adsorption of gold, they were found to be deformed after four consecutive adsorption/desorption cycles (*cf.* Fig. 3d–i).

Conclusions

Two novel polymers, **Mac-DMP** and **Mac-TMP**, constructed from tetralactam macrocycles, namely, **Mac-DM** and **Mac-TM**, were designed and synthesized, and their gold adsorption capabilities were investigated. Nitrogen sorption analysis of the two polymers showed that **Mac-DMP** exhibits a larger BET surface area than **Mac-TMP**. FE-SEM and HRTEM images revealed that both polymers **Mac-DMP** and **Mac-TMP** exhibit different morphologies, that is, long fibers and spheres, respectively. While the presence of macrocycles assists in the selective encapsulation of gold ions from among other metal ions, it emerges that the interaction of heteroatoms and aromatic rings extant to the polymers with the gold ions evidently facilitates the capture of the latter in the pores of the polymers. Based on ICP-MS analyses, the amounts of gold adsorbed by the polymers, that is, **Mac-DMP** and **Mac-TMP**, were deter-

mined to be 1.27 and 0.72 g g^{-1} with 96 and 94% efficiencies, respectively. The binding of Au ions by the polymers was established by a number of techniques that include PXRD, XPS, elemental mapping, and HAADF imaging. It was further shown that the gold ions can be extracted from e-waste such as PCBs and that the amount extracted can be assayed by ICP-MS analyses. The polymers adsorb Pd^{2+} ions as well from the solution of mixed metal ions, albeit with less efficiency, that is, 51 and 47% by **Mac-DMP** and **Mac-TMP**, respectively. These results demonstrate the potential of macrocyclic metal ion-binding receptor-based POPs as inextricable materials for the capture of precious metal ions from e-waste.

Author contributions

J. N. M. was responsible for conceptualization, supervision, writing – review & editing and funding acquisition.

Data availability

Synthesis and characterization of compounds, TGA, solid-state ^{13}C NMR spectra of polymers, XPS, elemental mapping, DFT-optimized structure, and ^{1}H and ^{13}C NMR spectral reproductions are available in the ESI.†

Conflicts of interest

The authors declare no conflicts of interest.

Acknowledgements

A.K. gratefully acknowledges the Council of Scientific and Industrial Research (CSIR), New Delhi for the CSIR research associate fellowship (Project No. 09/092(1053)/2020-EMR-I). G. A. thankfully acknowledges the University Grants Commission (UGC), New Delhi for a research fellowship. J.N.M. is thankful to the Science and Engineering Research Board (SERB), India, for generous financial support through the J.C. Bose Fellowship (SB/S2/JCB-52/2014).

References

1 B. Zhu, S. Gong and W. Cheng, *Chem. Soc. Rev.*, 2019, **48**, 1668–1711.
2 A. S. K. Hashmi, *Chem. Rev.*, 2007, **107**(7), 3180–3211.
3 S. Witzel, A. S. K. Hashmi and J. Xie, *Chem. Rev.*, 2021, **112**, 8868–8925.
4 S. J. Berners-Price and A. Filipovska, *Metallomics*, 2011, **3**, 863–873.
5 M.-C. Tang, M.-Y. Chan and V. W.-W. Yam, *Chem. Rev.*, 2021, **121**, 7249–7279.
6 E. Drost and J. Hausselt, *Interdiscip. Sci. Rev.*, 1992, **17**, 271–280.
7 J. Cui and L. Zhang, *J. Hazard. Mater.*, 2008, **158**, 228–256.
8 R. Rajesh, D. Kanakadhurga and N. Prabaharan, *Environ. Challenges*, 2022, **7**, 100507.
9 K. Huang, J. Guo and Z. Xu, *J. Hazard. Mater.*, 2009, **164**, 399–408.
10 H. Duan, K. Hou, J. Li and X. Zhu, *J. Environ. Manage.*, 2011, **92**, 392–399.
11 B. Ghosh, M. K. Ghosh, P. Parhi, P. S. Mukherjee and B. K. Mishra, *J. Cleaner Prod.*, 2015, **94**, 5–19.
12 Y. Hong, D. Thirion, S. Subramanian, M. Yoo, H. Choi, H. Y. Kim, J. F. Stoddartd and C. T. Yavuz, *Proc. Natl. Acad. Sci. U. S. A.*, 2020, **117**, 16174–16180.
13 A. Akcil, C. Erust, C. S. Gahan, M. Ozgun, M. Sahin and A. Tuncuk, *Waste Manage.*, 2015, **45**, 258–271.
14 M. L. Arrascue, H. M. Garcia, O. Horna and E. Guibal, *Hydrometallurgy*, 2003, **71**, 191–200.
15 B. Pangeni, H. Paudyal, M. Abe, K. Inoue, H. Kawakita, K. Ohto and B. B. Adhikari, *Green Chem.*, 2012, **14**, 1917–1927.
16 C. I. Park, J. S. Jeong and G. W. Cha, *Bull. Korean Chem. Soc.*, 2000, **21**, 121–124.
17 D. Jermakowicz-Bartkowiak, B. N. Kolarz and A. Serwin, *React. Funct. Polym.*, 2005, **65**, 135–142.
18 P. Duel, M. S. Gutierrez, P. Rodríguez, A. Leon, K. A. Lopez, J. Morey and M. N. Piña, *RSC Adv.*, 2018, **8**, 36123–36132.
19 N. F. Abd Razak, M. Shamsuddin and S. L. Lee, *Chem. Eng. Res. Des.*, 2018, **130**, 18–28.
20 M. S. Gutiérrez, K. A. López, J. Morey and M. N. Piña, *Materials*, 2020, **13**, 1086.
21 H. Wu, Y. Wang, C. Tang, L. O. Jones, B. Song, X. Y. Chen, L. Zhang, Y. Wu, C. L. Stern, G. C. Schatz, W. Liu and J. F. Stoddar, *Nat. Commun.*, 2023, **14**, 1284.
22 H. T. Fissaha, R. E. C. Torrejos, H. Kim, W. J. Chung and G. M. Nisola, *Microporous Mesoporous Mater.*, 2020, **305**, 110301.
23 D. T. Sun, N. Gasilova, S. Yang, E. Oveisi and W. L. Queen, *J. Am. Chem. Soc.*, 2018, **140**, 16697–16703.
24 M. Mon, J. Ferrando-Soria, T. Grancha, F. R. Fortea-Perez, J. Gascon, A. Leyva-Perez, D. Armentano and E. Pardo, *J. Am. Chem. Soc.*, 2016, **138**, 7864–7867.
25 V. V. Karve, T. Schertenleib, J. Espín, O. Trukhina, X. Zhang, M. X. Campins, T. Kitao, C. E. Avalos, T. Uemura and W. L. Queen, *ACS Appl. Mater. Interfaces*, 2021, **13**, 60027–60034.
26 T. Xue, T. He, L. Peng, O. A. Syzgantseva, R. Li, C. Liu, D. T. Sun, G. Xu, R. Qiu, Y. Wang, S. Yang, J. Li, J. R. Li and W. L. Queen, *Sci. Adv.*, 2023, **9**, eadg4923.
27 B. Wang, Y. Ma, W. Xu and K. Tang, *Langmuir*, 2022, **38**, 8954–8963.
28 S. Yang, T. Li, Y. Cheng, W. Fan, L. Wang, Y. Liu, L. Bian, C.-H. Zhou, L.-Y. Zheng and Q.-E. Cao, *ACS Sustainable Chem. Eng.*, 2022, **10**, 9719–9731.
29 H.-L. Qian, F.-L. Meng, C.-X. Yang and X.-P. Yan, *Angew. Chem., Int. Ed.*, 2020, **59**, 17607–17613.

30 L. Zhang, Q.-Q. Zheng, S.-J. Xiao, J.-Q. Chen, W. Jiang, W.-R. Cui, G.-P. Yang, R.-P. Liang and J.-D. Qiu, *Chem. Eng. J.*, 2021, **426**, 131865.
31 T. S. Nguyen, Y. Hong, N. A. Dogan and C. T. Yavuz, *Chem. Mater.*, 2020, **32**, 5343–5349.
32 L. Tan and B. Tan, *Chem. Soc. Rev.*, 2017, **46**, 3322–3356.
33 N. B. McKeown, *Polymer*, 2020, **202**, 122736.
34 D. Ramimoghadam, E. M. Gray and C. J. Webb, *Int. J. Hydrogen Energy*, 2016, **41**, 16944–16965.
35 C. Yadav, A. K. Sahoo and J. N. Moorthy, *ACS Appl. Nano Mater.*, 2022, **5**, 14296–14310.
36 C. Yadav, S. Payra and J. N. Moorthy, *J. Catal.*, 2022, **413**, 769–778.
37 J.-B. Xiong, D. D. Ban, Y. J. Zhou, H.-J. Du, A. W. Zhao, L. G. Xie, G.-Q. Liu, S. R. Chen and L. W. Mi, *Sci. Rep.*, 2022, **12**, 1–7.
38 Z. Li and Y. W. Yang, *Adv. Mater.*, 2022, **34**, 2107401.
39 C. Yadav, V. K. Maka, S. Payra and J. N. Moorthy, *ACS Appl. Polym. Mater.*, 2020, **2**, 3084–3093.
40 C. Eisen, L. Ge, E. Santini, J. M. Chin, R. T. Woodward and M. R. Reithofer, *Nanoscale Adv.*, 2023, **5**, 1095–1101.
41 F. Maleki, A. Ghaemi and G. Mir Mohamad Sadegh, *Environ. Prog. Sustainable Energy*, 2022, **42**, e13954, DOI: **10.1002/ep.13954**.
42 N. A. Dogan, Y. Hong, E. Ozdemir and C. T. Yavuz, *ACS Sustainable Chem. Eng.*, 2019, **7**, 123–128.
43 D. Abdullatif, A. Khosropour, A. Khojastegi, I. Mosleh, L. Khazdooz, A. Zarei and A. Abbaspourrad, *ACS Appl. Polym. Mater.*, 2023, **5**, 412–419.
44 Y. Su, K. I. Otake, J. J. Zheng, H. Xu, Q. Wang, H. Liu, F. Huang, P. Wang, S. Kitagawa and C. Gu, *Nat. Commun.*, 2024, **15**, 144.
45 Y. Su, B. Li, Z. Wang, A. Legrand, T. Aoyama, S. Fu, Y. Wu, K. I. Otake, M. Bonn, H. I. Wang and Q. Liao, *J. Am. Chem. Soc.*, 2024, **146**, 15479–15487.
46 Y. Su, K. I. Otake, J. J. Zheng, S. Horike, S. Kitagawa and C. Gu, *Nature*, 2022, **611**, 289–294.
47 C. Gu, N. Hosono, J. J. Zheng, Y. Sato, S. Kusaka, S. Sakaki and S. Kitagawa, *Science*, 2019, **363**, 387–391.
48 S. Wang, Z. Xie, D. Zhu, S. Fu, Y. Wu, H. Yu, C. Lu, P. Zhou, M. Bonn, H. I. Wang and Q. Liao, *Nat. Commun.*, 2023, **14**, 6891.
49 Y. Su, B. Li, H. Xu, C. Lu, S. Wang, B. Chen, Z. Wang, W. Wang, K. I. Otake, S. Kitagawa and L. Huang, *J. Am. Chem. Soc.*, 2022, **144**, 18218–18222.
50 Y. Su, Z. Wang, A. Legrand, T. Aoyama, N. Ma, W. Wang, K. I. Otake, K. Urayama, S. Horike, S. Kitagawa and S. Furukawa, *J. Am. Chem. Soc.*, 2022, **144**, 6861–6870.
51 Y. Su, K. I. Otake, J. J. Zheng, P. Wang, Q. Lin, S. Kitagawa and C. Gu, *Nat. Commun.*, 2024, **15**, 144.
52 R. Gomes and A. Bhaumik, *J. Solid State Chem.*, 2015, **222**, 7–11.
53 P. Chandrasekhar, A. Mukhopadhyay, G. Savitha and J. N. Moorthy, *Chem. Sci.*, 2016, **7**, 3085–3091.
54 A. Mukhopadhyay, V. K. Maka, G. Savitha and J. N. Moorthy, *Chem*, 2018, **4**, 1059–1079.
55 V. K. Maka, P. Tamuly, S. Jindal and J. N. Moorthy, *Appl. Mater. Today*, 2020, **19**, 100613.
56 S. Jindal and J. N. Moorthy, *Inorg. Chem.*, 2022, **61**, 3942–3950.
57 W. Liu, A. G. Oliver and B. D. Smith, *J. Am. Chem. Soc.*, 2018, **140**, 6810–6813.
58 J. J. Gassensmith, E. Arunkumar, L. Barr, J. M. Baumes, K. M. DiVittorio, J. R. Johnson, B. C. Noll and B. D. Smith, *J. Am. Chem. Soc.*, 2007, **129**, 15054–15059.
59 C. Gozalvez, J. L. Zafra, A. Saeki, M. Melle-Franco, J. Casado and A. Mateo-Alonso, *Chem. Sci.*, 2019, **10**, 2743–2749.
60 E. Arunkumar, C. C. Forbes, B. C. Noll and B. D. Smith, *J. Am. Chem. Soc.*, 2005, **127**, 3288–3289.
61 C. G. Collins, A. T. Johnson, R. D. Connell, R. A. Nelson, I. Murgu, A. G. Oliver and B. D. Smith, *New J. Chem.*, 2014, **38**, 3992–3998.
62 I. Murgu, J. M. Baumes, J. Eberhard, J. J. Gassensmith, E. Arunkumar and B. D. Smith, *J. Org. Chem.*, 2011, **76**, 688–691.
63 D.-H. Li and B. D. Smith, *J. Org. Chem.*, 2019, **84**, 2808–2816.
64 Y. Qiu, S. Yu, S. M. Wang, M. L. Liu, S. Y. Li, H. Yao, L. P. Yang and L. L. Wang, *Chem. Eng. J.*, 2024, **495**, 153143.
65 S. Dey, A. Kumar, D. Sain, H. P. Nayek, A. Hazra, S. Goswami, S. Jana, H.-K. Fun and S. Isik, *Lett. Org. Chem.*, 2015, **12**, 584–590.
66 S. K. Kundu and A. Bhaumik, *ACS Sustainable Chem. Eng.*, 2015, **3**, 1715–1723.
67 W. Xu, F. Wang, S. Chen, K. Zhang and K. Tang, *Sep. Purif. Technol.*, 2024, **328**, 125039.
68 T. Nakamura, Y. Mochidzuki and S. Sato, *J. Mater. Res.*, 2008, **23**, 968–974.
69 Y. Chen, Z. Li, R. Ding, T. Liu, H. Zhao and X. Zhang, *J. Hazard. Mater.*, 2022, **426**, 128073.
70 F. Wang, J. Zhao, M. Zhu, J. Yu, Y. S. Hu and H. Liu, *J. Mater. Chem. A*, 2015, **3**, 1666–1674.
71 T. Groenewald, *Hydrometallurgy*, 1976, **1**, 277–290.
72 B. Altansukh, G. Burmaa, S. Nyamdelger, N. Ariunbolor, A. Shibayama and K. Haga, *Int. J. Soc. Mater. Eng. Resour.*, 2014, **20**, 29–34.